The effect of the changes in chemical composition due to thermal treatment on the mechanical properties of Pinus densiflora

Peng, Qiushi; Spear, Morwenna; Ormondroyd, Graham; Chang, Wen-shao

Construction and Building Materials

DOI:
10.1016/j.conbuildmat.2022.129303

Published: 05/12/2022

Publisher's PDF, also known as Version of record

Construction and Building Materials 358 (2022) 129303

Contents lists available at ScienceDirect

Construction and Building Materials

journal homepage: www.elsevier.com/locate/conbuildmat

The effect of the changes in chemical composition due to thermal treatment on the mechanical properties of *Pinus densiflora*

Qiushi Peng [a], Graham Ormondroyd [b], Morwenna Spear [b], Wen-Shao Chang [a,*]

[a] School of Architecture, University of Sheffield, UK
[b] BioComposites Centre, Bangor University, UK

ARTICLE INFO

Keywords:
Wood Thermal-Treatment
Wood Chemical Composition
FTIR
Wood Mechanical Properties

ABSTRACT

Wood's chemical composition has a close relationship to its mechanical properties. Therefore, chemical analysis such as FTIR spectroscopy offers a reasonable non-destructive method to predict wood strength. Pine (*Pinus densiflora*) specimens were thermal-treated in different conditions (aerobic and anaerobic) and evaluated by 3-point bending test for modulus of rupture (MOR) and by FTIR spectroscopy for chemical composition. Density and moisture content changes were also assessed in this study. The result showed that both density and equilibrium moisture content at 20 °C with 65 % humidity change little at low treatment temperatures, but they decrease at high treatment temperatures and when treated in the presence of oxygen. The MOR was improved by the reactions that occurred, including cellulose crystallisation, lignin condensation and cross-linking, whereas it was decreased by degradation reactions. The MOR were well predicted by two FTIR peak at 1318 cm^{-1} (relating to CH_2 bond and condensation of G-ring of lignin), and at 1730 cm^{-1} (pertaining to changes to carbonyl groups in hemicelluloses) and density. It was concluded that FTIR spectroscopy provides a suitable method for wood non-destructive mechanical testing.

1. Introduction

Timber has a long history of being used in construction and has recently made a renaissance due to the declared climate emergency, the desire to utilise timber in construction and its ability to act as a carbon store [1,2]. However, a single member of a timber-framed structure might slowly lose mechanical durability over a very long time period and result in structural failure, but this is not easy to evaluate from visual observation. Hence, non-destructive methods to predict timber mechanical properties are needed.

The interaction between wood chemical composition and mechanical properties are discussed. Wood chemical composition and mechanical properties both change, which imply that wood chemical composition and mechanical properties are strongly correlated [3,4]. The tensile strength of wood is affected by the proportion of amorphous cellulose present, for example it has been shown to decrease dramatically after a large number of covalent bonds within the wood macromolecules were broken by a gamma irradiation treatment [5,6]. The author also demonstrated that longitudinal compressive strength and shear strength are affected by changes in the proportion of crystalline cellulose and the extent of lignin cross-linking [6]. Winandy and Rowell [7] clearly described the way that mechanical properties of wood result from the covalent bonds within the three main wood polymers (cellulose, hemicelluloses, and lignin), and the hydrogen bonds that occur within and between them. Hence, a relationship between wood chemical composition and mechanical properties is worthy of study.

Temperature effects are frequently studied as a tool to investigate various changes in wood, and many studies have investigated these effects by chemical and mechanical analysis [8,9]. Many researchers have shown that temperature can also alter the structural polymers of the wood [10,11]. A comprehensive review of the literature summarised that below 150 °C thermal treatment, both free and bound water evaporate, whilst at the temperatures between 150 °C and 250 °C, many kinds of chemical changes happen to the cellulose, hemicelluloses and lignin of wood [8]. The extent and type of changes are significantly affected by the treatment environment, such as the presence of oxygen, steam, or inert gases. Moreover, wood is carbonised and degraded, releasing various gases at higher temperatures greater than 250 °C. Wood has thermal shrinkage reaction at this temperature due to hemicellulose degradation [12].

Cellulose, hemicelluloses, and lignin are the main molecules in the wood cell wall. The cellulose microfibrils play a significant role in

* Corresponding author.
E-mail address: w.chang@sheffield.ac.uk (W.-S. Chang).

https://doi.org/10.1016/j.conbuildmat.2022.129303
Received 25 March 2022; Received in revised form 26 September 2022; Accepted 27 September 2022
Available online 20 October 2022

supporting the structure, whilst hemicelluloses and lignin form a matrix to enhance its integrity [7,13]. Cellulose is the most stable molecule of wood in any atmosphere or temperature, retaining its structure and strength even at 260 °C for a long period [14–16]. Moreover, thermal treatment under 250 °C can result in an apparent increase in the crystallinity of cellulose. Inert and moist atmospheres can lead to an increased change in the level of crystallinity compared to reactions in air or oxygenated environments [17–21]. Hemicelluloses are affected significantly during thermal treatment. At low temperatures, it condenses with lignin, whilst at high temperatures, it degrades to give shorter chain molecules, and evolving gaseous or liquid decomposition products, which are important factors in the observed mass loss [14,22–24]. Elastic moduli is reduced due to hemicelluloses degradation [12]. Lignin molecules have complex chemical reactions which vary according to temperature, treatment atmosphere and duration. Condensation, cross-linking, and degradation reactions can be observed in lignin molecules during thermal treatment. Treatments in inert atmospheres can enhance lignin condensation and cross-linking reactions [14,25], whereas the presence of oxygen and use of high temperatures lead to it undergoing significant degradation [26]. A long period thermal treatment (160 °C for 504 h) was shown to also caused serious degradation reactions in both hemicellulose and lignin [10]. However, the traditional chemical detection methods (quantitative wet chemical analysis) are not capable of distinguishing chemical changes in the structure of wood molecules, especially lignin [17,27,28]. An advanced technique, ATR-FTIR (attenuated total reflection Fourier transform infrared spectroscopy), is a quick and effective method for analysing the changes in chemical composition of wood and alterations to the prevalence of different functional groups during thermal degradation or reactions [29–31].

The MOE (Modulus of elasticity) and MOR (Modulus of rupture) are determined in bending tests for wood. For thermally treated woods, both are affected by treatment temperature and duration, and it is possible to select treatment conditions to optimise the MOR and MOE attained [16,32,33]. In addition, the oxygen content of the treatment atmosphere has a close negative correlations with MOE and MOR of the treated wood. Specifically, both the MOE and MOR of pine decreased in oxygen atmosphere treatments but experienced no significant changes in air and increased slightly in nitrogen atmospheres, where all treatments were conducted at 150 °C for 16 h [34]. Mass loss is also an important parameter correlating with the chemical changes affecting wood's mechanical properties after thermal treatment. Low mass loss (up to 4 %) has been shown to not affect the MOE and MOR significantly, whereas high mass loss is correlated with a dramatic decrease in both [16,32]. MOR changes is more significant than that of MOE during thermal treatment [35,36], especially in the longitudinal direction [12].

As many studies have proved that the changes of wood chemical composition and mechanical properties can be detected after thermal treatment, this research will use thermal treatment to cause changes, and detect chemical composition by ATR-FTIR and mechanical properties by 3-point bending test. The aim of the study is to predict wood mechanical properties by FTIR as a non-destructive test method for application in larger structural members. In fact, several non-destructive tests have been studied in wood mechanical properties evaluation such as colour measurement [37–39], wave-based method (Ultrasound, stress wave and Lamb wave) [40–43] and near infra-red (NIR) or FTIR spectrometry [44,45]. A recent data analysis method based on machine learning was exploited to improve prediction model significantly [38,43,46]. However, ATR-FTIR can show the chemical changes of wood molecules from the fingerprint region of spectra, hence the ATR-FTIR will be used in this study. Small samples will be used in experiment to permit full comparison of the treatment effects on the mechanical properties and spectroscopic observation to derive a model.

The changes to the molecular composition of the cellulose, hemicelluloses, and lignin of wood during thermal treatment are complex and have been discussed in many studies, some are summarised in Table 1. As a composite of different polymers, the wood mechanical properties are affected not only by the molecular weight of each component (cellulose, hemicelluloses, and lignin), but also by the distribution of these within the microfibrillar arrangement of the cell wall structure [47]. Only chemical reactions affecting the structural molecules are discussed in this study. Table 1 presents the main reactions seen during thermal treatments and how these correspond to changes in intensity of the peaks of the FTIR spectrum. Note that many of these are studies on pure compound, not the compound in the wood cell wall.

2. Materials and method

Pine specimens were from an approximately 30 years growing trunk and were taken out from the place close to the bark side, but sapwoods were not used in this experiment. The wood species was *Pinus densiflora* with each specimens containing both earlywood and latewood and the dimensions of 2 mm (tangential) × 4 mm (radial) × 40 mm (longitudinal) (Fig. 1) were used in the experiment.

Table 1
Chemical Functional Group Changes resulting from Thermal Treatment and Corresponding FTIR Peaks.

Chemical Reaction	Location	Name	Functional groups	FTIR peak absorption change	FTIR Peak (cm^{-1})
Crystallization[48]	Cellulose	Ether linkage	C—O—C	↑	Peak 1154
		Hydroxyl	C–OH	↑	Peak 1110
Deacetylation [49]	Hemicelluloses	Carbonyl	C═O	↓	Peak 1730
		Alkene	C═C	↑	Peak 1595
Hemicelluloses Degradation [50]	Hemicelluloses	Ester carbonyl	C═O	↑	Peak 1730
		Alkene	C═C	↑	Peak 1595
			Others	↓	Peak 1226 to 1507
Condensation I [51]	Lignin	Ether carbonyl	C—O—C	↓	Peak 1154
		-	C—C	↑	Peak 1054
Condensation II [52]	Lignin	Ether	C—O—C	↑	Peak 1154
		Hydroxyl	–OH	↓	Peak 3336
Cross-linking [9]	Lignin	Alkene	C═C	↓	Peak 1595
		Aromatic skeletal		↑	Peak 1507
		Carbonyl	C═O	↓	Peak 1730
Lignin Degradation [53,54]	Lignin	Hydroxyl	–OH	↓	Peak 3336
		Alkene	C═C	↑	Peak 1595
		-	C—C	↓	Peak 1054
		Aromatic skeletal		↓	Peak 1507
Lignin Dehydration [53]	Lignin	Hydroxyl	–OH	↓	Peak 3336
		Alkene	C═C	↑	Peak 1595
		-	C—H	↓	Peak 1025
Oxidation [55]	Lignin	Hydroxyl	–OH	↓	Peak 3336
	Hemicelluloses	Ketone	C═O	↑	Peak 1730

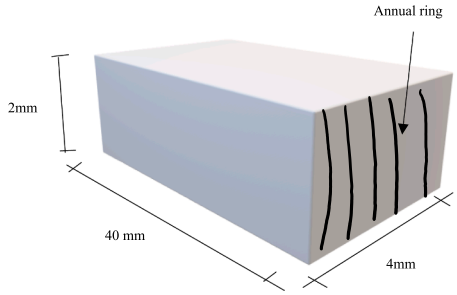

Fig. 1. Sample Size and Annual Ring Direction in the Experiment.

The temperature of the thermal treatment was set at 120 °C±5, 160 °C±5 and 200 °C±5 for 8, 12, 16, 20 and 24 h in air and vacuum atmospheres (Table 2). Each group contained 15 specimens. There were 465 specimens in total with a group of 15 untreated specimens as reference.

All the specimens were placed in a conditioning chamber with 20 °C and 65 % relative humidity for at least two weeks until the weight did not change any further then dried for approximately 24 h, again until the weight did not change, in a 105 °C oven to determine the value of EMC for the untreated wood prior to treatment. Thermal treatment was then started immediately on the oven dried specimens. Specimens were weighed after treatment, to determine the pure mass loss of wood due to the thermal treatment (excluding any moisture). The specimens were then placed back into the conditioning chambers and conditioned until no further mass change was seen before re-weighing, the EMC of the treated wood was determined using this data. The density of each specimen was measured at the same time. FTIR and 3-point bending tests were run after re-conditioning. The sequence of the experiment is shown in Fig. 2.

Table 2
FTIR Wavenumber and Corresponding Chemical Functional Groups of Wood.

No.	wavenumber	Compound
1	3336	O—H Stretch [57]
2	2910	CH– stretch in methyl- and methylene groups
	2882	CH– stretch in methyl- and methylene groups [58]
3	2103	Absorption caused by the ATR crystal
	1990	Absorption caused by the ATR crystal
4	1730	C═O stretching in unconjugated ketone, carbonyl, carboxylic acid and ester groups (frequently of carbohydrate origin) [58–61]
5	1642	–OH bending, affected by water absorption [62,63]
6	1595	C═C stretching of the aromatic ring; COO^- stretching [59,64]
7	1507	Aromatic skeletal vibration [59,62,64]
8	1456	C—H deformation stretching in CH_2 and CH_3, and aromatic skeletal vibrations [58,59]
9	1421	O—H in aromatic skeletal; C—H deformation stretching in CH_2 of cellulose [59,65]
10	1366	C—H bending in cellulose and hemicelluloses [65,66]
11	1330	Phenol group; –OH bond to aromatic hydrocarbon group [67,68]
12	1318	Condensation of guaiacyl unit (hardwood lignin) and syringyl unit [69] And CH_2 bending in cellulose [58,65]
13	1262	C—O of guaiacyl ring stretching (lignin) [59,62,70]
14	1226	C—C, C—O—C (lignin) [64]
15	1204	C—O—C or O—H in plane bending [71]
16	1154	Bridge C—O—C symmetric stretching in cellulose and noncellulosic polysaccharides [62,72]
17	1110	C-OH stretching [72,73]
18	1054	C—C and C—O stretching [72,73]
19	1025	C—H in-plane deformation and C—O stretching [58,73]
20	895	Anomeric vibration at β-glycosidic linkage [65,72]

Peak no.1–3 were shown in Fig. 4, peak no.4–20 were shown in Fig. 3.

2.1. Testing environment

All testing facilities were in a laboratory at 20 °C and 65 % relative humidity. The temperature and humidity were controlled by an automatic system for 24 h a day.

2.2. Vacuum oven

An oven with vacuum compressor was used to conduct the thermal treatment process. All valves were switched off and a continuously running compressor was used to create a vacuum environment below 5 Pa. For treatment in air, a through current of air was generated by opening the air inlet valve and setting the compressor at “low” running mode. The fresh heated air was drawn across the samples slowly as the oven temperature was not affected.

2.3. Mechanical testing

The mechanical properties were tested in 3-point bending mode using an Instron universal test machine. The span of the fixture was 28.5 mm and the cross-head speed was set at 0.025 mm/s.

2.4. ATR-FTIR spectroscopy

The spectra of the specimens were obtained by a THERMO Nicolet 8000 FTIR equipped with a PIKE GladiATR, a 45° single reflection ATR accessory with a 3.0 mm ZnSe based ATR crystals. Specimens were clamped in the ATR accessory and each specimen were scanned 15 times on a smooth surface. Raw FTIR spectra were processed by cubic spline baseline correction at 835 cm^{-1} 1850 cm^{-1} and 3800 cm^{-1} [29,56] by Essential FTIR software. According to Kocaefe, Poncsak and Boluk [9], thermal treatment was assumed not to affect C—H bond at 2910 cm^{-1}, so FTIR spectra were normalised to the peak at 2910 cm^{-1} after baseline correction. The FTIR spectrum is the result of the superimposing many peaks, so deconvolution of the peaks can be used to distinguish the area of each individual peak. Fig. 2 shows the peak fitting for pine specimens without any treatment. The raw FTIR spectrum (black) and cumulative peak fitting (red) coincide with R-square 0.998. The peak centre wavenumber and the corresponding functional groups of the molecules present in wood are shown in Table 2.

3. Results and discussion

3.1. Mass Loss, equilibrium moisture content and density change

Density and equilibrium moisture content (EMC) significantly correlated with wood’s mechanical properties [38,74–76], which were recorded comprehensively for this study. During thermal treatment, the mass loss in air was higher than under vacuum, whilst mass loss also increased with temperature and length of treatment period (Table 3). The highest mass loss (14.5 %) was seen for the treatment at 200 °C in air for 24 h, while in a vacuum under the same temperature and duration it was just 8.05 %. Oxygen is widely recognised as a significant parameter that promotes mass loss at this temperature [8]. At 160 °C and 120 °C, the mass loss for air treatment was slightly higher than under vacuum, standing at approximately 3 % and 2.2 %, respectively, and for vacuum treatment, the mass loss reduced to 2.98 % and 2.11 %. Thus, the oxygen present in air did not appear to affect mass loss significantly under such treatment for 24 h. Hemicellulose degradation and deacetylation reactions are the main reactions responsible for mass loss[14,77]. In the FTIR spectrum for 200 °C treatment, the large decrease in hydroxyl groups (overlapping peaks at 3336 cm^{-1} and 3360 cm^{-1}, Fig. 4) indicated the reactions on the hemicelluloses [17,23,27]. The peaks from 1226 cm^{-1} to 1507 cm^{-1} relating to lignin also had a significant reduction showing that lignin was also degraded in the 200 °C treatment (Fig. 4).

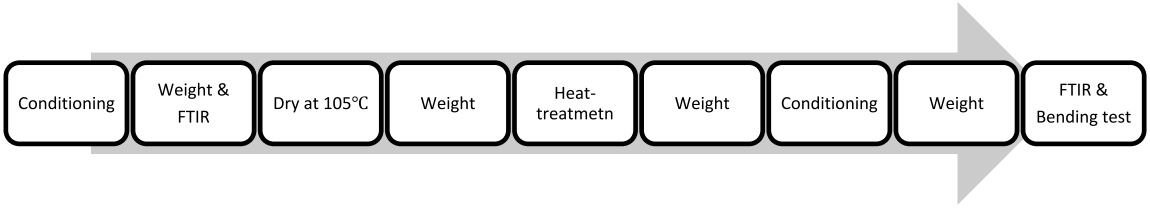

Fig. 2. Sequence of conditioning, measurement and treatment steps in the Experiment.

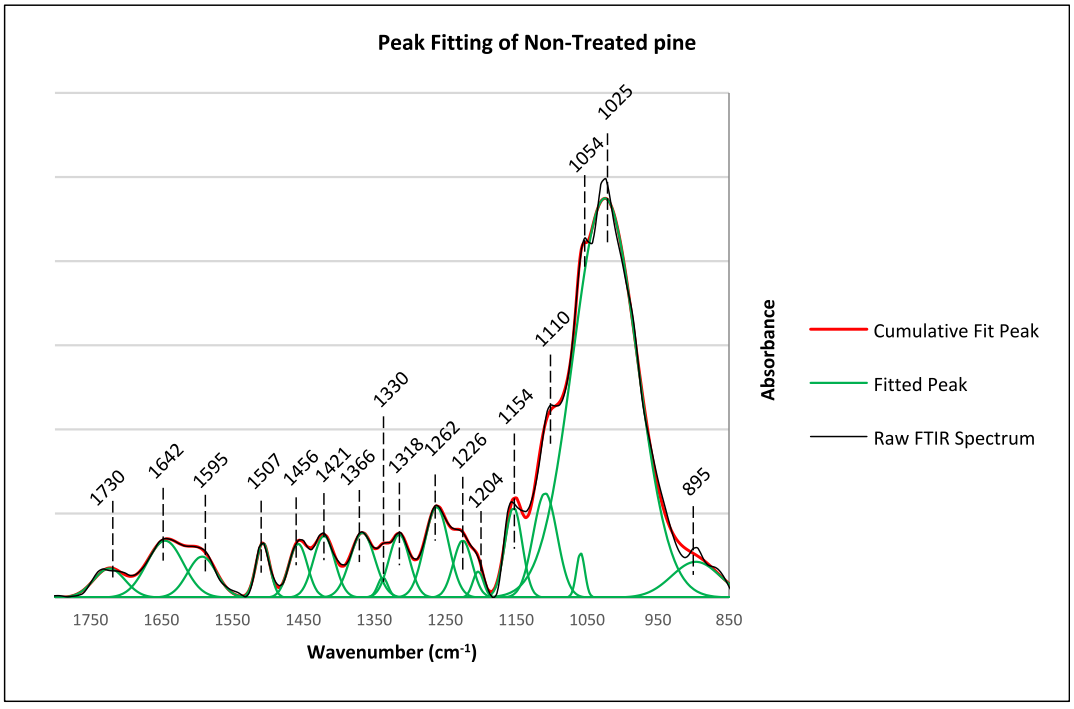

Fig. 3. Peak Fitting of Fingerprint Region of Un-treated Pine.

Table 3
Mass Loss of Wood As A % Of Initial Weight Of Wood From Thermal Treatment.

Mass loss	Control 0H (%)	Temperature (°C)		8 h (%)	12 h (%)	16 h (%)	20 h (%)	24 h (%)
air	0	120	Mean	1.1	1.4	1.9	2	2.3
			SD	0.15	0.12	0.09	0.36	0.24
		160	Mean	1.5	2	2.5	2.7	3.2
			SD	0.14	0.09	0.20	0.17	0.20
		200	Mean	6.3	10.6	11.9	12.9	14.5
			SD	0.96	1.29	0.73	1.35	1.62
vacuum		120	Mean	1.0	1.5	1.8	2.0	2.1
			SD	0.08	0.14	0.18	0.17	0.15
		160	Mean	1.0	2.4	2.5	2.7	3.0
			SD	0.40	0.12	0.14	0.12	0.09
		200	Mean	4.6	4.6	5.7	6.8	8.0
			SD	1.04	1.13	0.49	0.79	0.72

The EMC of untreated wood at 20 °C and 65 % relative humidity was 10.5 %, and only a small change was seen for the specimens treated at 120 °C thermal-treatment in air atmosphere (10.3 %) and in vacuum (10.2 %). The value of EMC decreased for specimens from higher temperature treatments and treatments in an oxygen atmosphere (Table 4). As with mass loss, the highest EMC decrease was observed for treatment at 200 °C in air after 24 h, decreasing from 10.5 % to 5.3 %, which was also reported by Straže et.al [78]. For all treatments, the reduction in EMC reached a maximum after the first 16 h treatment, with only small further changes seen for the longer treatments of 20 and 24 h. Jämsä and Viitaniemi [79] built a close relationship between the decrease of moisture content and the loss of hydroxyl groups. As mentioned above, the loss of hydroxyl functionalities is clearly seen in the FTIR spectrum (Fig. 4), at 3335 cm^{-1} and 3360 cm^{-1}, relating to the hydroxyl groups decreases.

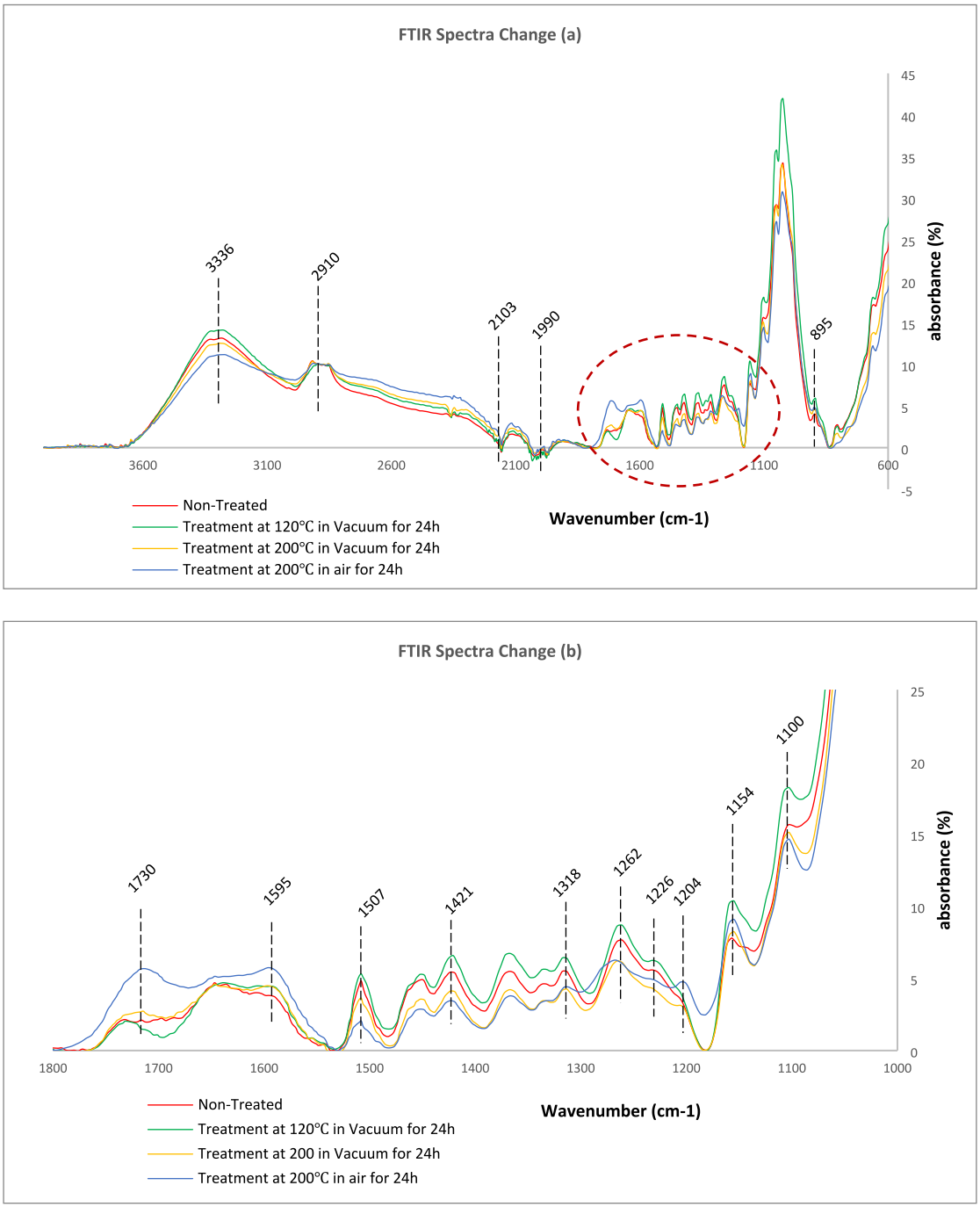

Fig. 4. FTIR Spectra of Non-treated Pine and 200 °C Treatment in Air and Vacuum for 24 Hours (a)full spectrum (b) fingerprint region.

3.2. *Mechanical property and chemical composition*

The Modulus of Rupture (MOR) for treatment at 120 °C in a vacuum constantly increases with time, reaching approximately 16 % increase after 24 h (Fig. 5). Similar results for thermal treatment were reported by other studies [16,34]. In the FTIR spectra of specimens treated in the same condition, the absorbance of bond C—O—C in cellulose and hemicelluloses (peak at 1154 cm^{-1}) was increased. As this bond can be used to analyse cellulose crystallinity [48], along with bonds at 1420 cm^{-1}, 1110 cm^{-1} and 895 cm^{-1}, relating to the bond of CH_2, C-OH and C—O—C (β-glycosidic linkage), we were able to confirm that cellulose crystallinity increased in the 120 °C vacuum treatment specimens, through the increase of these four peaks. The peak at 1507 cm^{-1}, correlating to aromatic skeletal vibration of lignin, also increased. This peak revealed condensation/cross-linking reaction in the lignin macromolecule, which was also an important factor that enhanced wood strength [9]. Similar lignin composition changes were also reported by other authors [26,77,80]. Lignin crosslinking reactions were observed, these are associated with a reduction of the 1595 cm^{-1} peak reducing the number of C═C bonds. In addition, a deacetylation reaction was observed due to the reduction the peak at 1730 cm^{-1}, for the C═O bonds within the ester carbonyl, similar results were reported by many other studies [20,23,77]. To sum up, the treatment at 120 °C in vacuum, includes an apparent increase in cellulose crystallisation, lignin condensation/cross-linking reactions and less than 3 % mass loss contribute to an improvement in wood strength. In the treatment at 120 °C in air, MOR increases in the first 16 h and then decreases. On the FTIR spectrum, condensation and cross-linking reactions were also observed

Table 4
EMC of Wood Specimens After Conditioning, Resulting From Thermal Treatment.

EMC	Control 0H (%)	Temperature (°C)		8 h (%)	12 h (%)	16 h (%)	20 h (%)	24 h (%)
air	10.5	120	Mean	10.1	10.0	10.1	10.1	10.3
	0.33		SD	0.35	0.33	0.37	0.34	0.49
		160	Mean	9.8	8.6	8.3	8.3	8.3
			SD	0.34	0.37	0.37	0.32	0.34
		200	Mean	8.2	6.2	5.3	5.4	5.6
			SD	0.36	0.14	0.21	0.26	0.27
vacuum		120	Mean	10.4	10.1	10.3	10.6	10.2
			SD	0.37	0.36	0.67	0.33	0.41
		160	Mean	10.3	8.7	8.6	8.5	8.5
			SD	0.40	0.37	0.40	0.36	0.43
		200	Mean	7.5	6.1	6.0	6.1	6.2
			SD	0.45	0.53	0.27	0.42	0.51

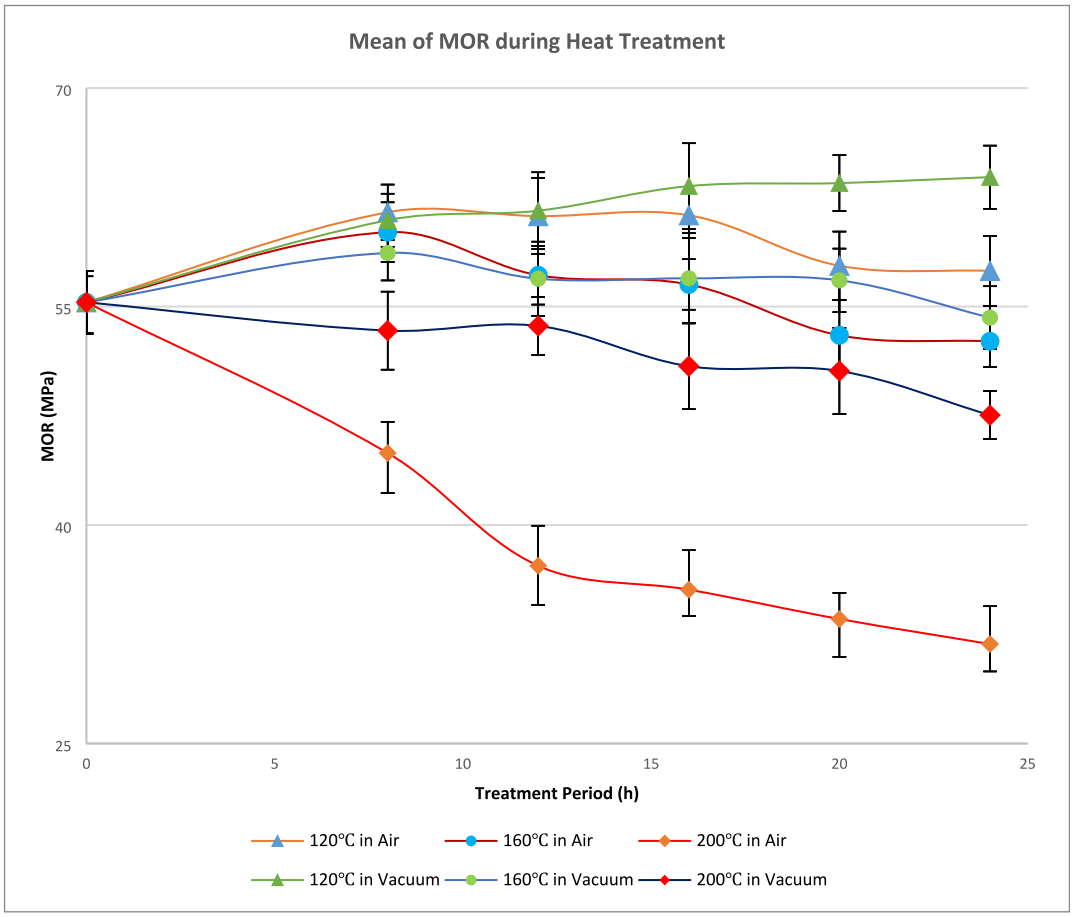

Fig. 5. MOR Changes During Thermal Treatment in Different Atmospheres.

by related peak changes, but to a lower degree. The presence of oxygen may inhibit crystallisation, condensation and cross-linking and leads to a bit more mass loss from the treatment.

Treatment at a temperature of 200 °C caused a steady decrease in MOR with increasing time, and for the 24 h treatments both in air and vacuum atmospheres, the decrease was approximately 42 % and 12 %, respectively. The mechanical strength decreasing more in air than in an inert atmosphere at 200 °C was also reported by others [6,32]. Regarding the FTIR spectra of the specimens treated in the air atmosphere, the peak at 3336 cm^{-1} relating to hydroxyl groups (–OH) of cellulose, hemicelluloses and lignin decreased significantly, which showed a large degradation in wood chemical components. The mass loss in Table 3 confirms this degradation. The peaks from 1507 cm^{-1} to 1318 cm^{-1}, relating to hemicelluloses and lignin, decreased significantly after the 24-hour treatment (Fig. 4), which was caused by the degradation and carboxylation of polysaccharides. The chemical reaction products contained many C═C bonds (peak at 1595 cm^{-1}), carboxylic acid and ester carbonyl groups (C═O, peak at 1730 cm^{-1}), C—O bonds (1262 cm^{-1}) and C—O—C bonds (1154 cm^{-1} and 1204 cm^{-1}), which can be observed as an increase in the 5 peaks (Fig. 4), similar result was reported by Wang, Fu and Lin [81]. Note that on the FTIR spectra, the peak at 1262 cm^{-1} appears to be lower than non-treated specimens, however, after deconvolution of peaks, the actual size of this peak increased, the apparent lower peak area arose because of dramatic changes in the intensity of neighbouring peaks. A remarkably similar result was reported by González-Peña and Hale [82] who reported that

MOR was negatively correlated with intensity of these five peaks in a study on thermal modification of spruce wood. However, one peak at 1517 cm^{-1} relating to aromatic skeletal vibrations, showed an increase in his study, but was not found in this study. Diffuse reflectance FTIR method maybe more sensitive than ATR method. The FTIR spectra of the specimens treated in vacuum at 200 °C showed few significant differences from the air treatment spectra described above. The main differences were on peak at 1730 cm^{-1}, 1262 cm^{-1} and 1204 cm^{-1}. The peak at 1730 cm^{-1} showed a slight increase, indicating that the presence of oxygen was involved in chemical reactions at 200 °C, some have reported this to be the formation of ketones or carboxylic acids during hemicellulose degradation [58,61] or formation of aldehyde groups in lignin [58]. Considering the smaller mass loss in vacuum compared to air, oxidation and degradation are likely to be the main reactions. In addition, cellulose crystallisation and lignin condensation/cross-linking may also happen in the first few hours of 200 °C treatment, according to Goroyias and Hale [83], who also observed a clear increase in MOR after 20 min. This was associated with increase of the peaks in this temperature treatment, and indicated that crystalised cellulose, the functional groups of C═O, C—O—C and C═C were the most stable part of wood molecule. The implication of this observation is that very short times at high temperature show trends which have similarity to the lower temperature treatments, but other mechanisms dominate the systems as treatment time is extended.

At 160 °C treatment, the changes are complex. The MOR of the specimens treated in air and vacuum both increased in the first few hours of treatment but decreased at longer durations. On the FTIR spectra, cellulose crystallisation and lignin condensation/cross-linking were observed mainly in the first 12 h treatment, which enhanced the MOR as discussed for the 120 °C treatments. Degradation dominated at longer durations and caused a reduction in the wood strength, with similar molecular changes to those discussed for 200 °C treatment. Consequently, MOR was improved with cellulose crystallisation and lignin condensation/cross-linking, but decreases with degradation, which also contribute to a density decrease, oxygen was an important factor promoting degradation. The equivalence of time and temperature in determining the intensity of treatment, and mass loss, within thermal modification of wood are well explored [84].

The modulus of elasticity (MOE) underwent a complex set of changes in the experiment especially between 8 and 20 h treatment (Fig. 6). After 24 h treatment, the MOE increased by approximately 12 %, 2 % and 2 % at 120 °C 160 °C and 200 °C respectively in a vacuum, but changed by approximately 3 %, 1 % and −5% at 120 °C, 160 °C and 200 °C in air treatment. The presence of oxygen was again correlated with a negative influence on MOE, as seen for the MOR data, but with some differences. The MOE increased in all treatments for the first 8 h, and the highest increase even happens at 200 °C in air, being 6 % with 6–8 % mass loss. The FTIR spectra show significant cellulose crystallisation due to the increase of peak at 1154 cm^{-1} and 1110 cm^{-1}, which might be an underlying factor for this MOE enhancement. The changes of MOE are less than MOR during the thermal-treatment, which was also reported by other studies [35,36]. One reason is that MOE change is not significant before 8 % mass loss [85] and another reason is that the wood cell structure also plays a close role in determining the stiffness of wood (MOE) [47,86,87]. Since the thermal treatment did not affect cell structure, the changes in MOE were not as large as MOR.

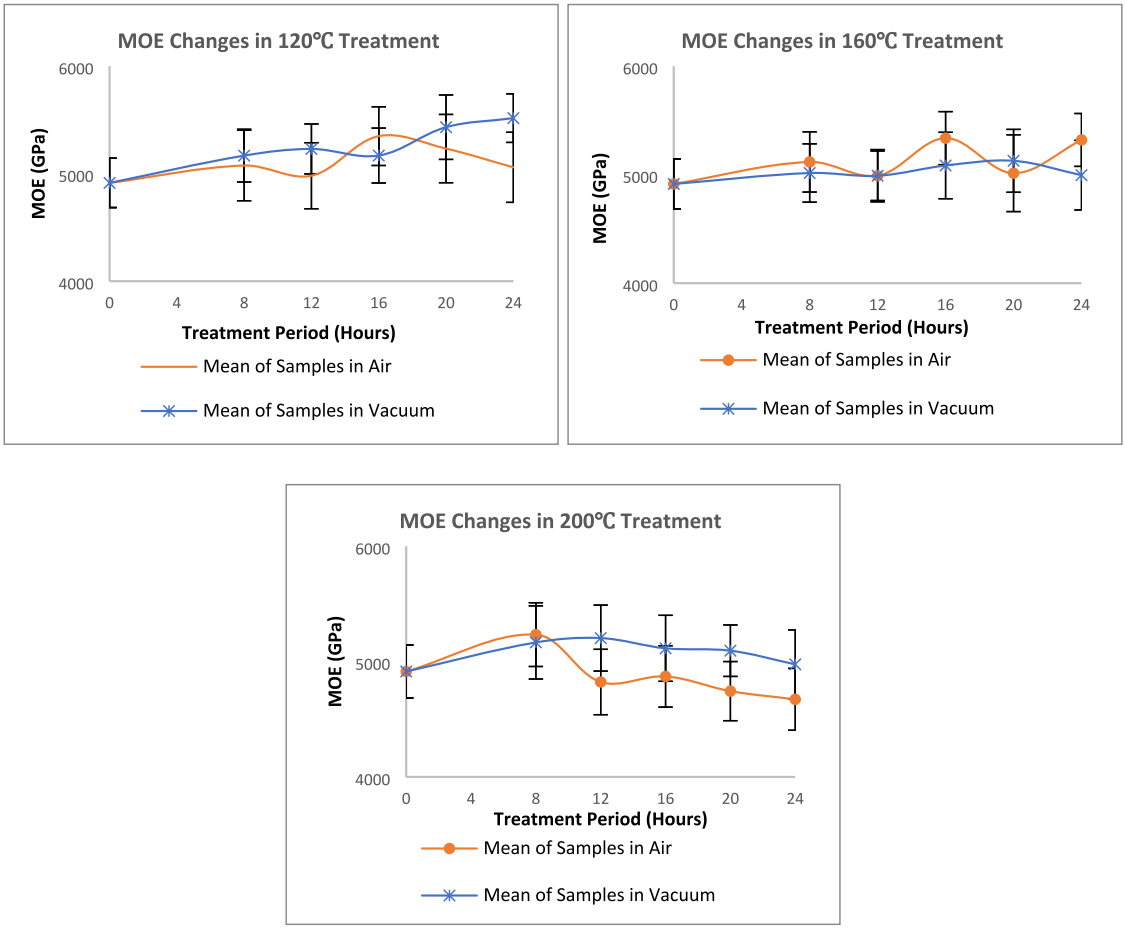

Fig. 6. Plot of MOE with Treatment Duration, Showing Scatter Within Raw Data And Trend for Mean Values.

3.3. MOR prediction though the FTIR spectrum

Density has close relationship to the mechanical properties of wood and can be used as a parameter to predict MOR [86,88]. However, in this study several changes were detected using FTIR that showed that more factors play a significant role in the mechanical properties, especially during thermal treatments. The ratio of strength-to-density after treatment was plotted (Fig. 7), and several trends were observed with treatment temperature (Fig. 7a) and atmosphere (Fig. 7b). Note that the datasets include specimens from all treatment durations. It is assumed that specimens with higher mass loss have lower density within these datasets, but we acknowledge that there is considerable scatter in the density values, relating to the natural variability of initial density of the specimens prior to treatment. The gradient of the MOR-Density plot was the highest after 200 °C treatment in any treatment atmosphere, and for the treatment at 160 °C and 120 °C (Fig. 7a), the gradient tended to be smaller. The absence of oxygen also inhibited strength loss, so the gradient tended to be lower than for the air atmosphere population (Fig. 7b).

The FTIR data was also considered. Pearson correlation analysis shows that the highest positive and negative correlation with MOR is seen for the peaks at 1318 cm^{-1} with 0.797 and 1730 cm^{-1} with −0.824 (Table 5), which related to the bond of CH_2 and condensation of lignin guaiacyl unit, and the ester carbonyl group (C═O), respectively. Table 1 indicated that the 1318 cm^{-1} peak for CH_2 units and condensation of the phenolic rings in lignin was closely related to condensation and cross-linking reactions with positive correlation and degradation (decomposition) with negative correlation. The carbonyl group (C═O) was also connected to a positive correlation with degradation and a negative correlation to lignin cross-linking and deacetylation (Table 1). Fig. 8 shows the change of the two peaks during thermal treatment. Hence, a ratio of the peak size of 1318 cm^{-1} and 1730 cm^{-1} can be used to quantify chemical changes, and it is expected that it can be used with the density data to predict MOR. In Fig. 9, the relationship between the MOR and density (ρ) × Ratio of Peak1318/Peak 1730 ($R_{1318/1730}$) was a natural logarithmic base.

In fact, nonlinear curve fit (by OriginPro software, equation (1)) and multiple regression analysis (by SPSS software, equation (2)) method calculated the regression model to predict MOR.

$$\sigma = 27.21878 \times \rho \times \left(\ln \frac{Wv_{1318}}{Wv_{1730}} + 5.41234\right) \quad (1)$$

$$\sigma = 10.608 + 101.764 \times \rho + 0.032 \times Wv_{1318} - 0.016 \times Wv_{1730} \quad (2)$$

where σ is the MOR, ρ is the density, whilst Wv_{1318} and Wv_{1730} are the sizes of peaks 1318 cm^{-1} and 1730 cm^{-1}. Both R-Square (coefficient of determination) and Adjusted R-Square of the equation I are 0.753. For the equation II, the R-Square (coefficient of determination) and Adjusted R-Square are 0.75 and 0.749, respectively, and without the problem of multicollinearity. Both methods indicated that the predicted MOR is highly matched to the measured one. The relationships between measured MOR and predicted MOR were shown in Fig. 10.

MOE cannot so easily be predicted on the basis of density and the ratio of peak sizes. According to Astley, Stol and Harrington [89], wood MOE has a close relationship to the cell geometries. Yang and Evans [88] also produced a regression model to predict MOE by density and MFA (microfibril angle). Hence, the regression model could be improved significantly if this factor was incorporated, but it will not be discussed in this study due to lack of data.

However, few further studies should be conducted. Firstly, wood is an anisotropic materials, its mechanical properties are different in three dimensions. This study only illustrated the effects of wood's chemical

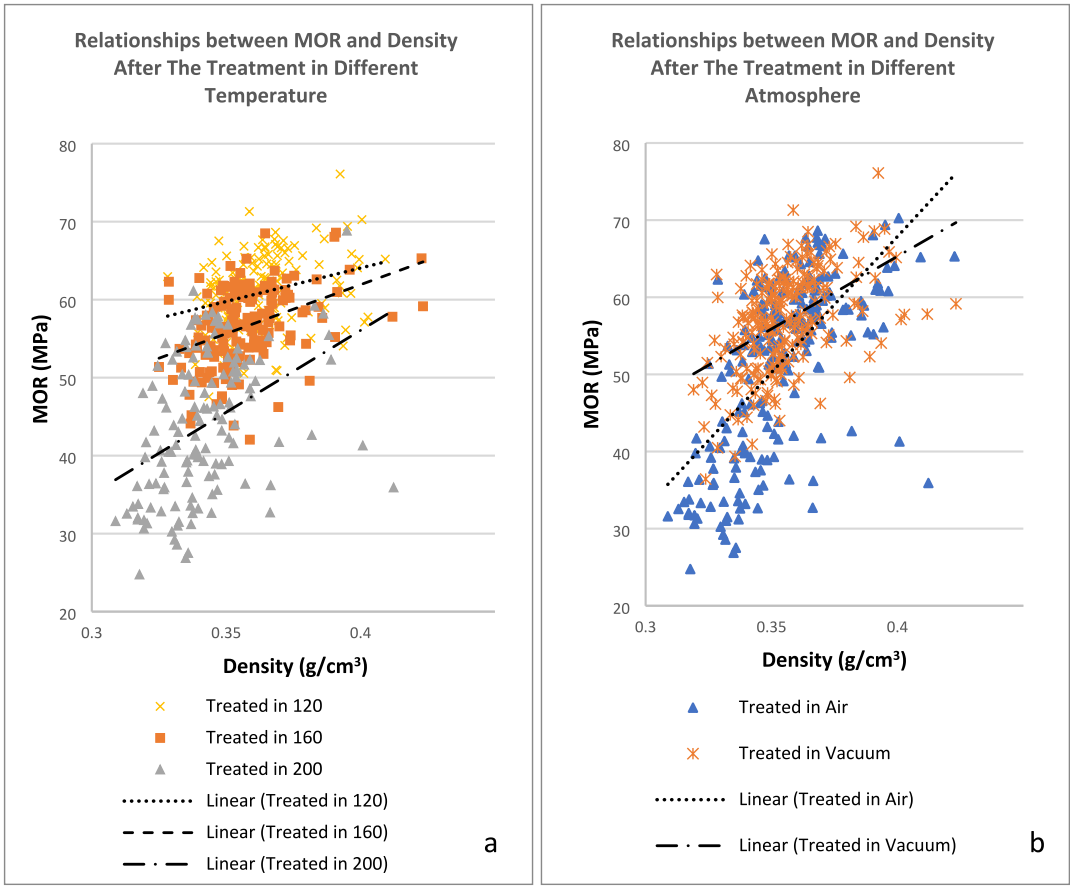

Fig. 7. Relationship Between MOR and Density After Different Treatment.

Table 5
Pearson Correlation of MOR-Peak Size.

MOR	Peak (cm-^{1})	1318	1335	1366	1421	1456	1507	1595	1642	1730
	Pearson Correlation	0.797**	-0.511**	0.477**	0.456**	0.527**	0.652**	-0.777**	0.717**	-0.824**
	Peak (cm^{-1})	**95**	**1025**	**1054**	**1110**	**1154**	**1204**	**1226**	**1262**	
	Pearson Correlation	0.084	-0.503**	-0.495**	0.292**	-0.548**	-0.722**	-0.018	-0.567**	

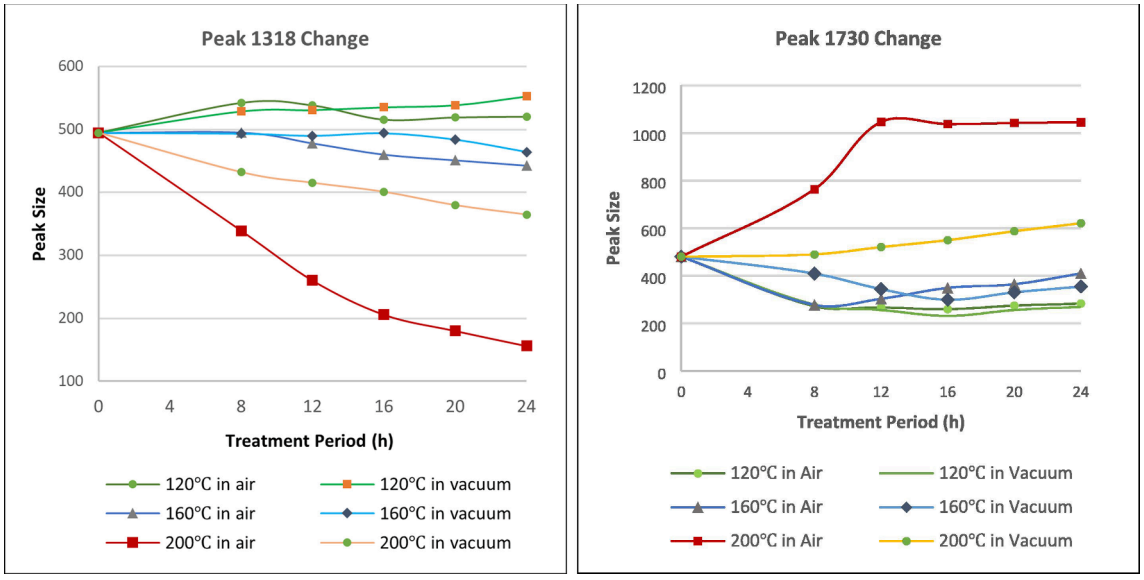

Fig. 8. FTIR Peak Size Changes of Peak 1318 cm^{-1} and 1730 cm^{-1} during Thermal Treatment.

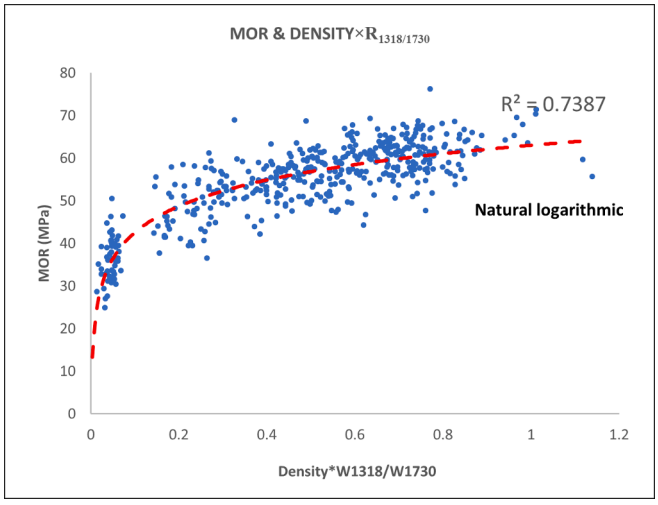

Fig. 9. Relationship Between MOR and Density × $R_{1318/1730}$.

composition in the mechanical properties in bending in the longitudinal direction, and the prediction model was only fitted with longitudinal MOR. The effects on other two directions should be studied. Secondly, the mathematic prediction model of wood mechanical properties worked well on the new *Pinus densiflora* wood. The model was unknown to predict the mechanical properties of ancient wood and other wood species, which would be prospective for further research. Finally, the mechanical properties were tested in the clear small wood specimens with the dimension of 2 mm × 4 mm × 40 mm, which cannot represent standard mechanical properties of structural elements. The aim of this phase of the study was to establish correlations on which to develop a model, and further work is needed to address how these trends related to structural timbers. The relationship between wood specimen size and its mechanical properties was studied that small clear specimens have higher MOR value while large scale specimens have greater MOE value due to wood defects such as knots [90,91].

4. Conclusion and outlook

A complex set of chemical composition changes are caused in wood by thermally induced reactions that occur in aerobic and anaerobic atmospheres. The relationship between the resulting chemical composition and the Modulus of Rupture (MOR) has been thoroughly investigated, with the following being elicited.

- Equilibrium moisture content (EMC) and density after treatment decrease with treatment temperature and decrease further for reactions in the presence of oxygen. Oxidation/condensation and degradation reactions are responsible for the decrease.
- Cellulose crystallisation, and lignin condensation and cross-linking reactions in wood molecules improve the MOR at lower temperatures or shorter times. Mass loss, caused by degradation or deacetylation, contributed to an MOR decrease at higher temperatures and longer treatment times.
- MOE changes in a complex manner during thermal treatment. Initial crystallisation, condensation and cross-linking improve MOE significantly, for conditions of up to 8 % mass loss. Beyond this mass loss, a decrease in MOE is seen. In addition, wood cell structure is also an essential factor affecting MOE.
- The FTIR peak at 1318 cm^{-1}, which is affected by condensation and degradation, and the peak 1730 cm^{-1}, which is affected by deacetylation and degradation of the hemicelluloses, but also formation of aldehydes in lignin during thermal reactions. The ratio of these two peaks ($R_{1318/1730}$) can be used to predict the MOR of small clear specimens when combined with wood density value.

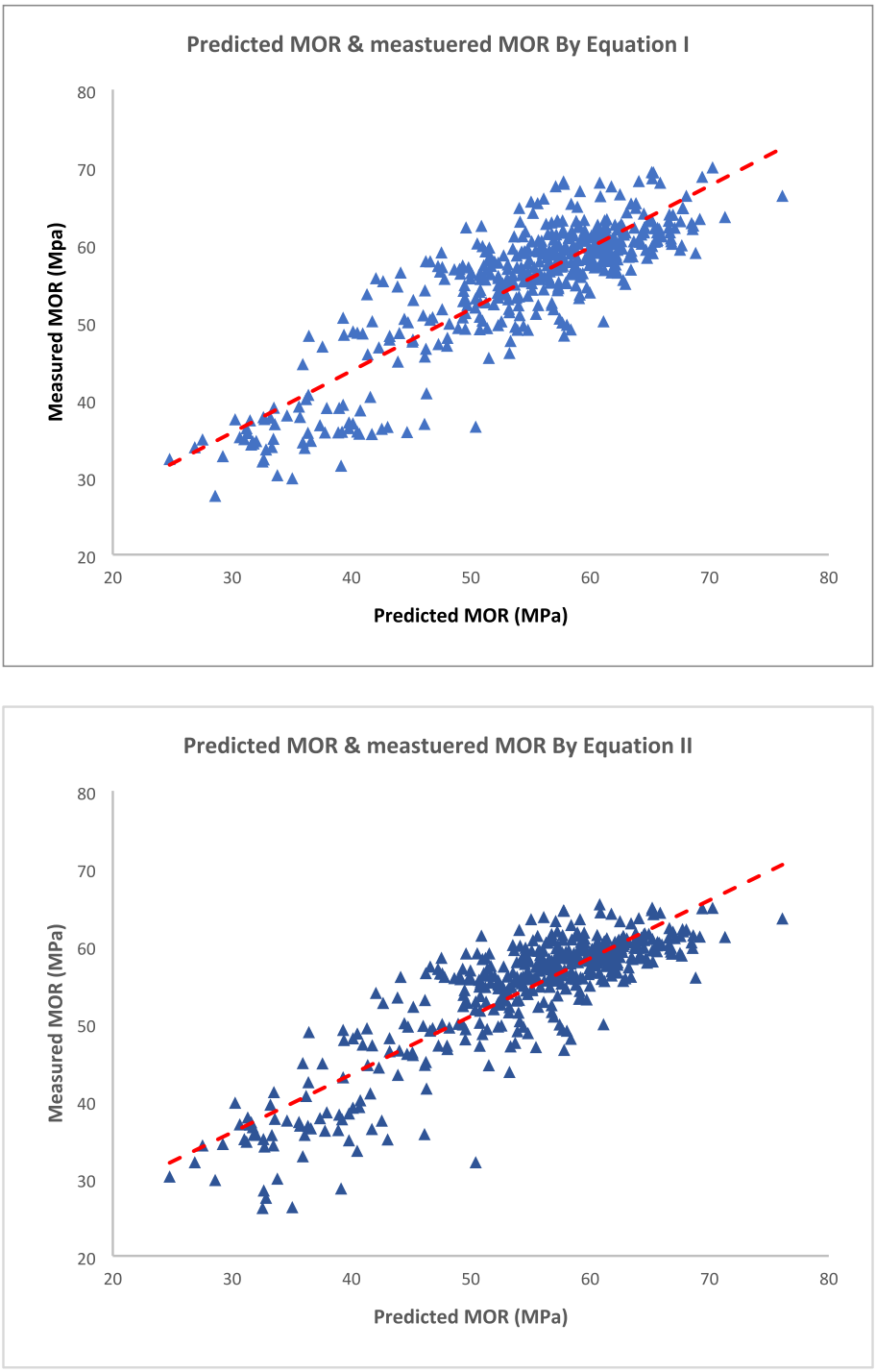

Fig. 10. Relationship Between the Predicted MOR and Measured MOR by Equation (1) and (2).

CRediT authorship contribution statement

Qiushi Peng: Software, Investigation, Data curation, Writing – original draft, Visualization, Validation. **Graham Ormondroyd:** Conceptualization, Resources, Methodology, Supervision. **Morwenna Spear:** Investigation, Methodology, Writing – review & editing. **Wen-Shao Chang:** Conceptualization, Methodology, Writing – review & editing, Supervision.

Declaration of Competing Interest

The authors declare that they have no known competing financial interests or personal relationships that could have appeared to influence the work reported in this paper.

Data availability

Data will be made available on request.

References

[1] R.H. Falk, Wood as a sustainable building material, Wood handbook: wood as an engineering material: chapter 1. Centennial ed. General technical report FPL; GTR-190. Madison, WI: US Dept. of Agriculture, Forest Service, Forest Products Laboratory: 2010 p. 1.1-1.6. 190 (2010).

[2] G. Ormondroyd M. Spear S. Curling Modified wood: review of efficacy and service life testing Proceedings of the Institution of Civil Engineers-Construction Materials 168 4 2015 187 203.
[3] D. Fengel, Aging and fossilization of wood and its components, Wood Sci. Technol. 25 (3) (1991) 153–177.
[4] A. Cavalli, D. Cibecchini, M. Togni, H.S. Sousa, A review on the mechanical properties of aged wood and salvaged timber, Constr. Build. Mater. 114 (2016) 681–687.
[5] J. Dinwoodie, Timber—a review of the structure-mechanical property relationship, J. Microsc. 104 (1) (1975) 3–32.
[6] M.J. Boonstra, J. Van Acker, B.F. Tjeerdsma, E.V. Kegel, Strength properties of thermally modified softwoods and its relation to polymeric structural wood constituents, Annals of Forest Science 64 (7) (2007) 679–690.
[7] J. Winandy, R. Rowell, The chemistry of wood strength, Advances in chemistry series (1984).
[8] B. Esteves, H. Pereira, Wood modification by heat treatment: a review, BioResources 4 (1) (2008) 370–404.
[9] D. Kocaefe, S. Poncsak, Y. Boluk, Effect of thermal treatment on the chemical composition and mechanical properties of birch and aspen, Bioresources 3 (2) (2008) 517–537.
[10] M.-C. Popescu, J. Froidevaux, P. Navi, C.-M. Popescu, Structural modifications of Tilia cordata wood during heat treatment investigated by FT-IR and 2D IR correlation spectroscopy, J. Mol. Struct. 1033 (2013) 176–186.
[11] S. Korkut, M. Akgül, T. Dündar, The effects of heat treatment on some technological properties of Scots pine (Pinus sylvestris L.) wood, BioResources 99 (6) (2008) 1861–1868.
[12] T. Adibaskoro, M. Makowska, A. Rinta-Paavola, S. Fortino, S. Hostikka, Elastic modulus, thermal expansion, and pyrolysis shrinkage of norway spruce under high temperature, Fire Technol. 57 (5) (2021) 2451–2490.
[13] J. Dinwoodie, Timber: its nature and behaviour, CRC Press, 2002.
[14] J. Bourgois, R. Guyonnet, Characterization and analysis of torrefied wood, Wood Science and Technology 22 (2) (1988) 143–155.
[15] S. Yildiz, E.D. Gezer, U.C. Yildiz, Mechanical and chemical behavior of spruce wood modified by heat, Build. Environ. 41 (12) (2006) 1762–1766.
[16] B. Esteves, A.V. Marques, I. Domingos, H. Pereira, Influence of steam heating on the properties of pine (Pinus pinaster) and eucalypt (Eucalyptus globulus) wood, Wood Science and Technology 41 (3) (2007) 193–207.
[17] M.J. Boonstra, B. Tjeerdsma, Chemical analysis of heat treated softwoods, Holz Als Roh-Und Werkstoff 64 (3) (2006) 204–211.
[18] M. Pétrissans, P. Gérardin, M. Serraj, Wettability of heat-treated wood, Holzforschung 57 (3) (2003) 301–307.
[19] M.T.R. Bhuiyan, N. Hirai, Study of crystalline behavior of heat-treated wood cellulose during treatments in water, Journal of Wood Science 51 (1) (2005) 42–47.
[20] H. Sivonen, S.L. Maunu, F. Sundholm, S. Jamsa, P. Viitaniemi, Magnetic resonance studies of thermally modified wood, Holzforschung 56 (6) (2002) 648–654.
[21] H. Wikberg, S.L. Maunu, Characterisation of thermally modified hard- and softwoods by C-13 CPMAS NMR, Carbohydr. Polym. 58 (4) (2004) 461–466.
[22] R. Alen, R. Kotilainen, A. Zaman, Thermochemical behavior of Norway spruce (Picea abies) at 180–225 degrees C, Wood Sci. Technol. 36 (2) (2002) 163–171.
[23] J.J. Weiland, R. Guyonnet, Study of chemical modifications and fungi degradation of thermally modified wood using DRIFT spectroscopy, Holz Als Roh-Und Werkstoff 61 (3) (2003) 216–220.
[24] M. Nuopponen, T. Vuorinen, S. Jämsä, P. Viitaniemi, Thermal Modifications in Softwood Studied by FT-IR and UV Resonance Raman Spectroscopies, J. Wood Chem. Technol. 24 (1) (2005) 13–26.
[25] A. Zaman, R. Alen, R. Kotilainen, Thermal behavior of scots pine (Pinus sylvestris) and silver birch (Betula pendula) at 200–230 degrees C, Wood Fiber Sci. 32 (2) (2000) 138–143.
[26] E. Windeisen, C. Strobel, G. Wegener, Chemical changes during the production of thermo-treated beech wood, Wood Science and Technology 41 (6) (2007) 523–536.
[27] B. Esteves, J. Graca, H. Pereira, Extractive composition and summative chemical analysis of thermally treated eucalypt wood, Holzforschung 62 (3) (2008) 344–351.
[28] B.F. Tjeerdsma, H. Militz, Chemical changes in hydrothermal treated wood: FTIR analysis of combined hydrothermal and dry heat-treated wood, Holz Als Roh-Und Werkstoff 63 (2) (2005) 102–111.
[29] L.M. Fahey, M.K. Nieuwoudt, P.J. Harris, Predicting the cell-wall compositions of Pinus radiata (radiata pine) wood using ATR and transmission FTIR spectroscopies, Cellulose 24 (12) (2017) 5275–5293.
[30] J.P. McLean, G. Jin, M. Brennan, M.K. Nieuwoudt, P.J. Harris, Using NIR and ATR-FTIR spectroscopy to rapidly detect compression wood in Pinus radiata, Canadian Journal of Forest Research-Revue Canadienne De Recherche Forestiere 44 (7) (2014) 820–830.
[31] C. Zhou, W. Jiang, B.K. Via, O. Fasina, G. Han, Prediction of mixed hardwood lignin and carbohydrate content using ATR-FTIR and FT-NIR, Carbohydr. Polym. 121 (2015) 336–341.
[32] F. Mburu, S. Dumarçay, J.F. Bocquet, M. Petrissans, P. Gérardin, Effect of chemical modifications caused by heat treatment on mechanical properties of Grevillea robusta wood, Polym. Degrad. Stab. 93 (2) (2008) 401–405.
[33] Y. Kubojima, T. Okano, M. Ohta, Vibrational properties of heat-treated green wood, J. wood science 46 (1) (2000) 63–67.
[34] P.H. Mitchell, Irreversible property changes of small loblolly pine specimens heated in air, nitrogen, or oxygen, Wood Fiber Sci. 20 (3) (1988) 320–335.
[35] P. Bekhta, P. Niemz, Effect of high temperature on the change in color, dimensional stability and mechanical properties of spruce wood, Holzforschung 57 (5) (2003) 539–546.
[36] G.-H. Kim, Effect of heat treatment on the decay resistance and the bending properties of radiata pine sapwood, Mater. Organismen 32 (2) (1998) 101–108.
[37] P. Torniainen, C.-M. Popescu, D. Jones, A. Scharf, D. Sandberg, Correlation of studies between colour, structure and mechanical properties of commercially produced thermowood® treated norway spruce and scots pine, Forests 12 (9) (2021) 1165.
[38] Z. Xin, D. Ke, H. Zhang, Y. Yu, F. Liu, Non-destructive evaluating the density and mechanical properties of ancient timber members based on machine learning approach, Constr. Build. Mater. 341 (2022), 127855.
[39] D. Kačíková, F. Kačík, I. Čabalová, J. Ďurkovič, Effects of thermal treatment on chemical, mechanical and colour traits in Norway spruce wood, Bioresource Technology 144 (2013) 669–674.
[40] A.R.P. Mascarenhas, R.R. de Melo, A.S. Pimenta, D.M. Stangerlin, F.L. de Oliveira Corrêa, M.S.V. Sccoti, E.A. de Oliveira Paula, Ultrasound to estimate the physical-mechanical properties of tropical wood species grown in an agroforestry system, Holzforschung 75 (10) (2021) 879–891.
[41] R. Rodolfo de Melo, K.T. Barbosa, R. Beltrame, A.P. Acosta, A.S. Pimenta, A.R. P. Mascarenhas, Ultrasound to determine physical-mechanical properties of Eucalyptus camaldulensis wood, Wood Material Science & Engineering 16 (6) (2021) 407–413.
[42] D. Van Duong, D. Ridley-Ellis, Estimating mechanical properties of clear wood from ten-year-old Melia azedarach trees using the stress wave method, Eur. J. Wood Wood Prod. 79 (4) (2021) 941–949.
[43] H. Fathi, V. Nasir, S. Kazemirad, Prediction of the mechanical properties of wood using guided wave propagation and machine learning, Constr. Build. Mater. 262 (2020), 120848.
[44] L. Schimleck, J. Matos, R. Trianoski, J. Prata, Comparison of methods for estimating mechanical properties of wood by NIR spectroscopy, J. Spectroscopy 2018 (2018).
[45] A. Sandak, J. Sandak, M. Riggio, Estimation of physical and mechanical properties of timber members in service by means of infrared spectroscopy, Constr. Build. Mater. 101 (2015) 1197–1205.
[46] V. Nasir, H. Fathi, A. Fallah, S. Kazemirad, F. Sassani, P. Antov, Prediction of mechanical properties of artificially weathered wood by color change and machine learning, Materials 14 (21) (2021) 6314.
[47] S. Fortino, P. Hradil, L.I. Salminen, F. De Magistris, A 3D micromechanical study of deformation curves and cell wall stresses in wood under transverse loading, J. Mater. Sci. 50 (1) (2015) 482–492.
[48] F. Carrillo, X. Colom, J. Sunol, J. Saurina, Structural FTIR analysis and thermal characterisation of lyocell and viscose-type fibres, Eur. Polym. J. 40 (9) (2004) 2229–2234.
[49] X. Zhou, W. Li, R. Mabon, L.J. Broadbelt, A Critical Review on Hemicellulose Pyrolysis, Energy Technology (2016).
[50] P.R. Patwardhan, R.C. Brown, B.H. Shanks, Product distribution from the fast pyrolysis of hemicellulose, ChemSusChem 4 (5) (2011) 636–643.
[51] V. Hemmilä, S. Adamopoulos, O. Karlsson, A. Kumar, Development of sustainable bio-adhesives for engineered wood panels–A Review, Rsc Advances 7 (61) (2017) 38604–38630.
[52] C. Liu, S. Wu, H. Zhang, R. Xiao, Catalytic oxidation of lignin to valuable biomass-based platform chemicals: A review, Fuel Process. Technol. 191 (2019) 181–201.
[53] H. Kawamoto, S. Horigoshi, S. Saka, Pyrolysis reactions of various lignin model dimers, J. wood science 53 (2) (2007) 168–174.
[54] M. Broda, C.-M. Popescu, Natural decay of archaeological oak wood versus artificial degradation processes—An FT-IR spectroscopy and X-ray diffraction study, Spectrochimica Acta Part A: Molecular and Biomolecular Spectroscopy 209 (2019) 280–287.
[55] M.D. Kärkäs, B.S. Matsuura, T.M. Monos, G. Magallanes, C.R. Stephenson, Transition-metal catalyzed valorization of lignin: the key to a sustainable carbon-neutral future, Org. Biomol. Chem. 14 (6) (2016) 1853–1914.
[56] J. Guo, H. Zhou, J.S. Stevanic, M. Dong, M. Yu, L. Salmén, Y. Yin, Effects of ageing on the cell wall and its hygroscopicity of wood in ancient timber construction, Wood Sci. Technol. 52 (1) (2018) 131–147.
[57] T. Kondo, The assignment of IR absorption bands due to free hydroxyl groups in cellulose, Cellulose 4 (4) (1997) 281.
[58] R.A. Kotilainen, T.J. Toivanen, R.J. Alen, FTIR monitoring of chemical changes in softwood during heating, J. Wood Chem. Technol. 20 (3) (2000) 307–320.
[59] K. Harrington, H. Higgins, A. Michell, Infrared spectra of Eucalyptus regnans F. Muell. and Pinus radiata D. Don Holzforschung-International Journal of the Biology, Chemistry, Physics and Technology of Wood 18 (4) (1964) 108–113.
[60] B. Barker, N.L. Owen, Identifying softwoods and hardwoods by infrared spectroscopy, J. Chem. Educ. 76 (12) (1999) 1706.
[61] S.-Z. Chow, Infrared spectral characteristics and surface inactivation of wood at high temperatures, Wood Sci. Technol. 5 (1) (1971) 27–39.
[62] R. Marchessault, Application of infra-red spectroscopy to cellulose and wood polysaccharides, Pure Appl. Chem. 5 (1–2) (1962) 107–130.
[63] D. Fengel, G. Wegener, Wood: chemistry, ultrastructure, Reactions 613 (1984) 1960–1982.
[64] O. Faix Classification of lignins from different botanical origins by FT-IR spectroscopy Holzforschung-International Journal of the Biology, Chemistry, Physics and Technology of Wood 45 s1 1991 21 28.
[65] P. Evans, A. Michell, K. Schmalzl, Studies of the degradation and protection of wood surfaces, Wood Sci. Technol. 26 (2) (1992) 151–163.

[66] C. Liang, R. Marchessault, Infrared spectra of crystalline polysaccharides. II. Native celluloses in the region from 640 to 1700 cm.− 1, Journal of Polymer Science 39 (135) (1959) 269–278.
[67] K.V. Sarkanen, C.H. Ludwig, Liguins, Occurrence, formation, structure, and reactions (1971).
[68] R. Marchessault, C. Liang, The infrared spectra of crystalline polysaccharides. VIII. Xylans, J. Polymer Science 59 (168) (1962) 357–378.
[69] C.S. Lancefield, S. Constant, P. de Peinder, P.C. Bruijnincx, Linkage Abundance and Molecular Weight Characteristics of Technical Lignins by Attenuated Total Reflection-FTIR Spectroscopy Combined with Multivariate Analysis, ChemSusChem 12 (6) (2019) 1139–1146.
[70] K.K. Pandey, A study of chemical structure of soft and hardwood and wood polymers by FTIR spectroscopy, J. Appl. Polym. Sci. 71 (12) (1999) 1969–1975.
[71] F.S. Parker, Applications of infrared, Raman, and resonance Raman spectroscopy in biochemistry, Springer Science & Business Media, 1983.
[72] G. Müller, C. Schöpper, H. Vos, A. Kharazipour, A. Polle, FTIR-ATR spectroscopic analyses of changes in wood properties during particle-and fibreboard production of hard-and softwood trees, BioResources 4 (1) (2009) 49–71.
[73] H. Higgins, C. Stewart, K. Harrington, Infrared spectra of cellulose and related polysaccharides, J. polymer science 51 (155) (1961) 59–84.
[74] E. Missanjo, J. Matsumura, Wood density and mechanical properties of Pinus kesiya Royle ex Gordon in Malawi, Forests 7 (7) (2016) 135.
[75] C. Gerhards, Effect of moisture content and temperature on the mechanical properties of wood: an analysis of immediate effects, Wood Fiber Sci. 14 (1) (2007) 4–36.
[76] D.E. Kretschmann, D.W. Green, Modeling moisture content-mechanical property relationships for clear southern pine, Wood fiber science 28 (3) (2007) 320–337.
[77] B.F. Tjeerdsma, M. Boonstra, A. Pizzi, P. Tekely, H. Militz, Characterisation of thermally modified wood: molecular reasons for wood performance improvement, Holz Als Roh-Und Werkstoff 56 (3) (1998) 149–153.
[78] A. Straže, G. Fajdiga, B. Gospodarič, Nondestructive Characterization of Dry Heat-Treated Fir (Abies Alba Mill.) Timber in View of Possible Structural Use, Forests 9 (12) (2018) 776.
[79] S. Jämsä, P. Viitaniemi, Heat treatment of wood–Better durability without chemicals, Proceedings of special seminar held in Antibes, France, 2001.
[80] G. Ucar, D. Meier, O. Faix, G. Wegener, Analytical pyrolysis and FTIR spectroscopy of fossil Sequoiadendron giganteum (Lindl.) wood and MWLs isolated hereof, Holz als Roh-und Werkstoff 63 (1) (2005) 57–63.
[81] D. Wang, F. Fu, L. Lin, Molecular-level characterization of changes in the mechanical properties of wood in response to thermal treatment, Cellulose (2022) 1–12.
[82] M.M. González-Peña, M.D. Hale, Rapid assessment of physical properties and chemical composition of thermally modified wood by mid-infrared spectroscopy, Wood Sci. Technol. 45 (1) (2011) 83–102.
[83] G. Goroyias, M. Hale, Heat treatment of wood strands for OSB production: Effect on the mechanical properties, water absorption and dimensional stability, International Research Group Wood Pre, Section 4-Processes (2002).
[84] O. Allegretti, I. Cuccui, N. Terziev, L. Sorini, A model to predict the kinetics of mass loss in wood during thermo-vacuum modification, Holzforschung 1(ahead-of-print) (2020).
[85] H. Rusche Thermal-degradationof wood at temperatures up to, 200 DEGREES C. 1. STRENGTH PROPERTIES OF DRIED WOOD AFTER HEAT-TREATMENT Holz als Roh-und Werkstoff 31 7 1973 273 281.
[86] R. Evans, J. Elic, Rapid prediction of wood stiffness from microfibril angle and density, Forest products journal 51 (3) (2001).
[87] R. Evans, J. Ilic, C. Matheson, Rapid estimation of solid wood stiffness using SilviScan, Proceedings of 26th Forest Products Research Conference: Research developments and industrial applications and Wood Waste Forum, Clayton, Victoria, Australia, 19-21 June 2000, CSIRO Forestry and Forest Products, 2000, pp. 49-50.
[88] J.L. Yang, R. Evans, Prediction of MOE of eucalypt wood from microfibril angle and density, Holz als Roh- und Werkstoff 61 (6) (2003) 449–452.
[89] R.J. Astley, K.A. Stol, J.J. Harrington, Modelling the elastic properties of softwood, Holz als Roh- und Werkstoff 56 (1) (1998) 43–50.
[90] A.M. Jamil, J.M. Zamin, M.M. Omar, Relationship between mechanical properties of structural size and small clear specimens of timber, J. Trop. For. Sci. (2013) 12–21.
[91] C.J. Cunha, M. Tenório, D. Lima, A.S. Rebouças, L.C. Neves, J.M. Branco, Mechanical Characterization of Iroko Wood Using Small Specimens, Buildings (2021).